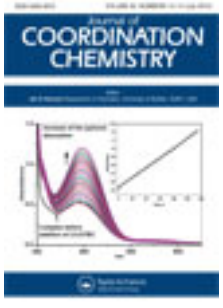

Journal of Coordination Chemistry
Publication details, including instructions for authors and subscription information:
http://www.tandfonline.com/loi/gcoo20

Magneto-structural study and synthesis optimization of a phosphovanadate copper complex, $[Cu(VO)_2(PO_4)_2(H_2O)_4]_n$

R. Baggio [a], D. Contreras [b], Y. Moreno [b], R. Arrue [b], I.E. Paulus [c], O. Peña [d] & J.Y. Pivan [d]

[a] Departamento Física, Comisión Nacional de Energía Atómica, Buenos Aires, Argentina

[b] Facultad de Ciências Químicas, Universidad de Concepción, Concepción, Chile

[c] Fachbereich Chemie, Philipps-Universität Marburg, Marburg, Germany

[d] Institut des Sciences Chimiques de Rennes, Université de Rennes-1, Rennes Cedex, France

Accepted author version posted online: 15 May 2012.Published online: 29 May 2012.

To cite this article: R. Baggio, D. Contreras, Y. Moreno, R. Arrue, I.E. Paulus, O. Peña & J.Y. Pivan (2012) Magneto-structural study and synthesis optimization of a phosphovanadate copper complex, $[Cu(VO)_2(PO_4)_2(H_2O)_4]_n$, Journal of Coordination Chemistry, 65:13, 2319-2331, DOI: 10.1080/00958972.2012.693608

To link to this article: http://dx.doi.org/10.1080/00958972.2012.693608

Journal of Coordination Chemistry
Vol. 65, No. 13, 10 July 2012, 2319–2331

Magneto-structural study and synthesis optimization of a phosphovanadate copper complex, $[Cu(VO)_2(PO_4)_2(H_2O)_4]_n$

R. BAGGIO†, D. CONTRERAS‡, Y. MORENO*‡, R. ARRUE‡, I.E. PAULUS§, O. PEÑA¶ and J.Y. PIVAN¶

†Departamento Física, Comisión Nacional de Energía Atómica, Buenos Aires, Argentina
‡Facultad de Ciências Químicas, Universidad de Concepción, Concepción, Chile
§Fachbereich Chemie, Philipps-Universität Marburg, Marburg, Germany
¶Institut des Sciences Chimiques de Rennes, Université de Rennes-1, Rennes Cedex, France

(*Received 12 January 2012; in final form 28 March 2012*)

The optimized synthesis of a phospho-vanadyl compound, $[Cu(VO)_2(PO_4)_2(H_2O)_4]_n$, is presented and its structural analysis is performed and discussed in relation to magnetic properties. The structure consists of a 2-D skeleton parallel to (100), made up by two independent VO_6 octahedra linked by phosphates. Neighboring 2-D structures stack along [100] and are connected by aqua-mediated H-bonds. The spatial disposition of paramagnetic ions gives rise to weak antiferromagnetic behavior, with $J = -17\,cm^{-1}$, which is consistent with a model of three paramagnetic centers in an irregular triangular arrangement. An optimization of the synthesis process, looking for a response surface with optimum experimental values, was performed using a multivariate analysis.

Keywords: Magneto-structural study; Phosphovanadate; Copper complex

1. Introduction

Open frameworks have received special attention because of their importance in different areas of Physics and Chemistry, such as ion exchange [1], catalysis [2], magnetism [3–5], etc. Much of this work is referred to open frameworks in which organic or complex units are inserted in the structure in a "guest–host" relation [6], thus giving place to hybrid compounds [7]. Among these systems, those with V–O–P units have received considerable attention [7, 8].

Our interest in vanadyl phosphates stems from the possibility of linking their coordination polyhedra in order to create 1-D, 2-D, or 3-D host structures. Phosphorus and vanadium can share oxygen atoms and give quite interesting arrangements [9–12]; while the coordination of phosphorus remains tetrahedral, V can adopt tetrahedral, square pyramidal, or octahedral coordination geometries [13].

2-D compounds presenting basic anionic layers of $[(V^{IV}O)(PO_4)]_n^-$ (A), $[(V^{V}O_2)(HPO_4)]_n^-$ (B), etc., which can undergo intercalation reactions are of particular

*Corresponding author. Email: ymoreno@udec.cl

ISSN 0095-8972 print/ISSN 1029-0389 online
http://dx.doi.org/10.1080/00958972.2012.693608

interest [9–15]. In addition, these frameworks can bind to other systems, such as metal complexes, and thus give hybrid compounds with a variety of interesting physical properties. In particular, magnetic coupling of metal centers can be achieved through this kind of architecture [16, 17].

Hydrothermal synthesis has played an important role in this kind of condensed system, which under normal conditions is not usually attainable [18, 19]. These compounds are obtained and studied without paying much attention to the efficiency of the reactions; in order to get a solid knowledge of the optimal experimental conditions, statistical methods are required. We have reported the use of a multivariate methodology (Chemometric) to optimize the synthesis of $[Cu(biqui)(H_2PO_4)_2]$. The general idea is to construct a response polynomial which describes the monocrystal amount synthesized, as a function of the experimental variables under analysis [20].

In this work we present some results arising from these ideas: the crystal structure of the inorganic 2-D compound $[Cu(PO_4)_2(VO)_2(H_2O)_4]$ (**1**), basically a layered structure of type (A), with intercalated CuO_6 octahedra, the analysis of the magnetic interactions between the paramagnetic centers in the structure and finally an optimization of experimental parameters in order to determine the best relation among time, reaction temperature, and reagents. Thus, a polynomial was obtained that describes the monocrystal amount obtained as a function of V_2O_5 concentration, reaction temperature, and cooling rate.

2. Experimental

Reagents were purchased from Sigma-Aldrich Inc. and used without purification. The synthesis was carried out in a 23 mL poly(tetrafluoroethylene)-lined stainless steel container under autogenous pressure. The reactants were stirred briefly before heating.

2.1. *Multivariate analyses*

In order to determine the conditions leading to a maximum amount of single crystals, the following reaction parameters were optimized: V_2O_5 mol (X_1), temperature (X_2), and cooling rate (°C h^{-1}) from 100°C (X_3). The variables which were kept fixed were the $Cu(NO_3)_2$ amount (1 m mol), pH (7.4), reaction time (36 h), cooling rate up to 100°C (2°C h^{-1}). The optimization was carried out through Response Surface Methodology (RSM). The aim of this analysis is to create a quadratic polynomial function. A Box–Behnken experimental design was used, made of a three-level factorial design and star points on a center of a hypercube [21]; the variable values are coded and normalized as a function of unitary values, −1 and +1. In our case, the values for X_1 ranged from 0.25 to 0.50, those for X_2 from 130°C to 150°C, and for X_3, from 1.0 to 4.0°C h^{-1}. In these ranges, the central point (coded 0) was set at 0.375 g for X_1, 140°C for X_2, and 2.5°C h^{-1} for X_3, being determined in triplicate to variance determinations. The response factor was the obtained crystal mass (mg) (Y).

A second-order function describing the system behavior was determined by a Multiple Linear Regression (MLR). The statistical validation was performed by an ANOVA test with 95% confidence. The optimal condition values were determined over

the response surface by the SIMPLEX method [22]. All the calculations were carried out using the Modde 7.0 software.

2.2. *Thermal analysis*

Thermogravimetric analysis (TGA) was performed on a crushed sample of manually selected crystals of $[Cu(VO)_2(PO_4)_2(H_2O)_4]_n$ using a Perkin Elmer TGA 7 thermogravimetric analyzer from 19°C to 600°C.

2.3. *Magnetic measurements*

The magnetic susceptibility (Quantum Design MPMS XL5 susceptometer) was measured at an applied field of 500 Oe (0.05 Tesla) between 2 and 300 K. Powder samples were placed and compacted inside a gelatin capsule. The temperature-independent magnetic contribution due to the sample holder was subtracted at all temperatures. The diamagnetic and other contributions due to the core electrons were estimated using Pascal constants and subtracted from the experimental values.

2.4. *X-ray diffraction*

Diffraction data were collected in a Bruker SMART AXS CCD diffractometer with graphite-monochromated Mo-Kα radiation ($\lambda = 0.71073$ Å). Semi-empirical absorption correction based on symmetry-equivalent reflections was applied. A total of 8994 reflections were collected, of which 3877 reflections were unique ($R_{int} = 0.057$). The structure was solved by direct methods and refined by full-matrix least-squares based on F^2. Structure solution, refinement, and generation of publication materials were performed with the use of the SHELXTL crystallographic software package [23–26]. The final refinement includes anisotropic displacement parameters for non-hydrogen atoms. The crystal data and structure refinement of $Cu(VO)_2(PO_4)_2(H_2O)_4$ are summarized in table 1.

3. Results and discussion

3.1. *Thermal analysis*

The thermal analysis is in agreement with the structural data for this compound (figure 1). The curve of $[Cu(VO)_2(PO_4)_2(H_2O)_4]_n$ shows three principal phenomena with weight loss in exothermic processes, ascribable to the loss of four water molecules. The first two losses at 246°C and 294°C correspond to one water molecule each (the small loss of water before 138°C is due to non-linked water molecules). The remaining two water molecules come out at 357°C. Therefore the thermal process involves: $[Cu(H_2O)_2(H_2O)(VOPO_4)_2H_2O] \rightarrow [Cu(H_2O)_2(VOPO_4)_2H_2O] + H_2O \rightarrow [Cu(H_2O)_2(VOPO_4)_2] + H_2O \rightarrow [Cu(VOPO_4)_2] + 2H_2O$.

Table 1. Crystal data for **1**.

Empirical formula	$Cu(VO)_2(PO_4)_2(H_2O)_4$
Formula weight	459.42
Temperature (K)	296
Wavelength (Å)	0.71073
Crystal system	Monoclinic
Space group	$P2_1/m$
Unit cell dimensions (Å, °)	
a	6.5910(18)
b	8.874(3)
c	9.069(2)
β	106.196(13)
Volume (Å^3), *Z*	509.4(2), 2
Absorption coefficient (mm^{-1})	4.26
Absorption correction	Multi-scan *SADABS* in *SAINT-NT* (Bruker, 2002) [24]
Crystal size (mm^3)	$0.32 \times 0.18 \times 0.14$
Reflections collected	3871
Independent reflections	1062 [R(int) = 0.045]
Observed reflections [$I > 2\sigma(I)$]	1045
Max. and min. transmission	0.79 and 0.89
Refinement method	Bruker Smart CCD area detector diffractometer
Data/restraints/parameters	1062/87/106
Goodness-of-fit on F^2	1.25
Final R indices [$I > 2\sigma(I)$]	$R_1 = 0.056$, $wR_2 = 0.151$
Largest difference peak and hole (e Å^{-3})	1.11 and −1.19

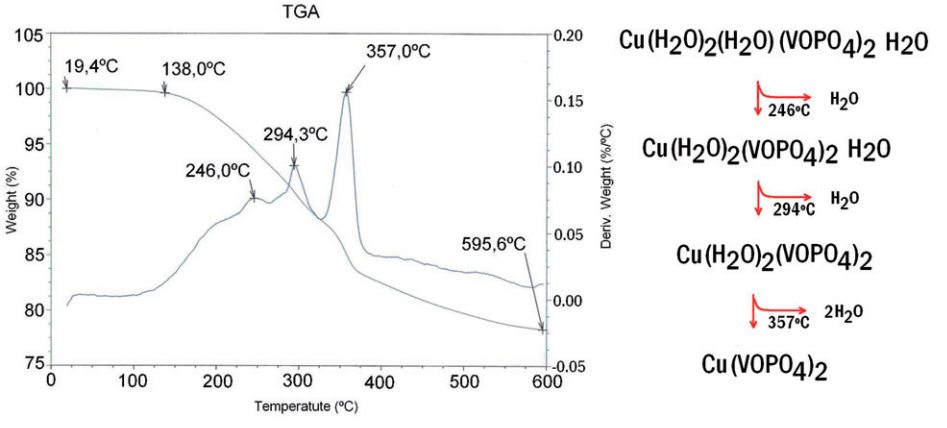

Figure 1. The TG and TD curves of $[Cu(VO)_2(PO_4)_2(H_2O)_4]_n$. The insert shows the thermal process.

3.2. *X-ray diffraction*

Figure 2 shows an ellipsoid plot of $[Cu(VO)_2(PO_4)_2(H_2O)_4]_n$. The asymmetric unit is composed of two different oxovanadium(IV) VO^{+2} moieties (V1–O1 and V2–O2) and a copper(II) cation, all laying on a mirror plane (and thus accounting for a net +3 charge), a full PO_4^{-3} (P1, O11, O12, O13, O14) in general position and three water molecules coordinated to one cation, two of them (O1W and O2W) also laying on a symmetry plane. The intricate coordination of the μ_5 phosphate leads to the three cations being six coordinate.

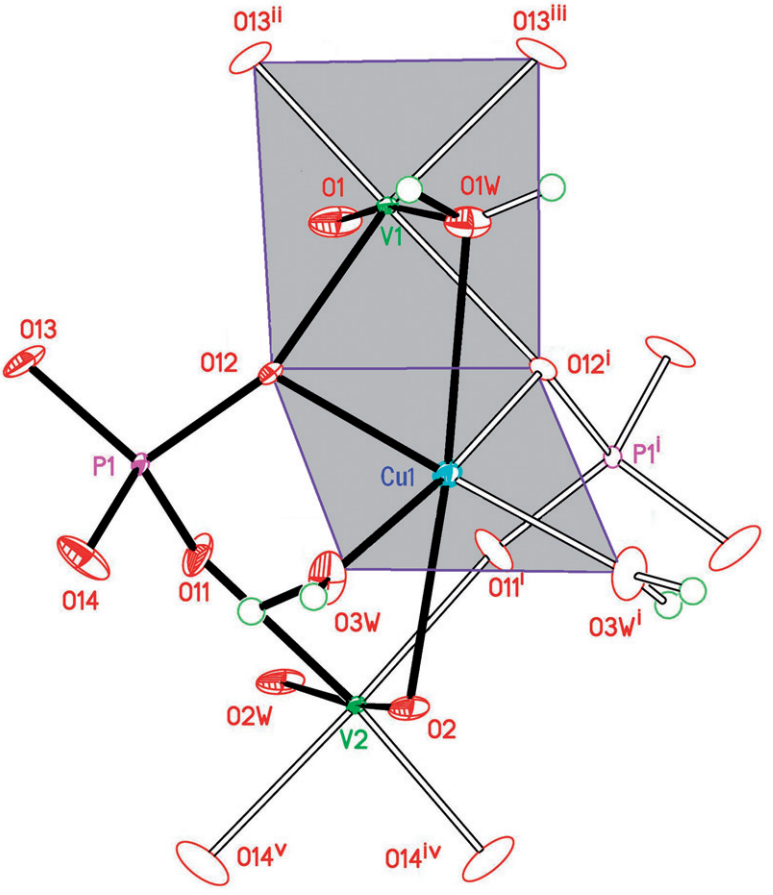

Figure 2. Ellipsoid plot (50% probability level) of $[Cu(VO)_2(PO_4)_2(H_2O)_4]_n$. Independent (symmetry-related) atoms are presented in heavy (hollow) bonds and filled (empty) ellipsoids. Symmetry codes: (i) $-x+2, y+1/2, -z+1$; (ii) $-x+2, y+1/2, -z+2$; (iii) $x, -y+1/2, z$; (iv) $-x+2, -y, -z+1$; (v) $-x+2, -y, -z+2$.

The Cu1 environment is a van der Waal's-deformed octahedron, with the basal plane provided by a phosphate oxygen (O12), a water (O3W), and their $[x, -y+1/2, z]$ symmetry-related counterparts. The apical sites are occupied by a second water molecule (O1W) and a vanadyl oxygen (O2), both at much longer distances (*ca* 20%) than basal ones (table 2). VO_6 octahedra are rather similar to each other in shape and metrics, with the planar base defined by phosphate oxygen atoms only (O12, $O12^{i}$, $O13^{ii}$, $O13^{iii}$, in the case of V1, and O11, $O11^{i}$, $O14^{iv}$, $O14^{v}$ for V2; see figure 2 and the corresponding caption for details). But contrasting to the Cu1 case, they present two very dissimilar apical bonds: a very short vanadyl one (V1–O1 and V2–O2) and very long, semicoordinated water molecule contacts (V1–O1W, V2–O2W; see table 2). The Cu1 and V1 octahedra share a face including the $O12\cdots O12^{i}$ edge, common to both basal planes and acting as a "hinge" between them (figure 2, shaded areas), defining a dihedral angle of 135.44(28)°. We shall comment on this below.

As stated, the structure can be envisaged as defined by a 2-D skeleton parallel to (100) and made up by two independent VO_6 octahedra linked by phosphates, or, in terms of

Table 2. Selected geometric parameters for **1** (Å, °).

Cu1–O3W	1.930(6)	V2–O2	1.609(8)
Cu1–O12	1.988(5)	V2–O11	1.983(6)
Cu1–O1W	2.394(8)	V2–O14^{iv}	1.996(6)
Cu1–O2	2.468(8)	P1–O13	1.512(6)
V1–O1	1.601(9)	P1–O14	1.530(6)
V1–O13^{iii}	1.961(6)	P1–O11	1.532(6)
V1–O12	2.046(6)	P1–O12	1.575(6)
V1–O1W	2.454(9)		
O3W^{i}–Cu1–O12	171.2(3)	O13^{iii}–V1–O12^{i}	91.2(2)
O1W–Cu1–O2	166.8(3)	O12–V1–O12^{i}	78.2(3)
O3W–Cu1–O3W^{i}	95.6(4)	O13^{iii}–V1–O1W	82.9(2)
O3W–Cu1–O12	91.5(2)	O12–V1–O1W	72.3(2)
O12–Cu1–O12^{i}	80.9(3)	O2–V2–O2W	175.8(3)
O3W–Cu1–O1W	107.9(2)	O11–V2–O14^{iv}	161.2(3)
O12–Cu1–O1W	74.6(2)	O2–V2–O11	98.0(3)
O3W–Cu1–O2	80.6(2)	O11–V2–O11^{i}	90.0(4)
O12–Cu1–O2	95.5(2)	O2–V2–O14^{iv}	100.7(3)
O1–V1–O1W	171.2(4)	O11–V2–O14^{v}	89.3(3)
O13^{iii}–V1–O12	155.0(2)	O14^{iv}–V2–O14^{v}	85.4(4)
O1–V1–O13^{iii}	103.2(3)	O11–V2–O2W	79.0(2)
O13^{ii}–V1–O13^{iii}	89.2(4)	O14^{iv}–V2–O2W	82.4(2)
O1–V1–O12	101.0(3)		

Symmetry codes: (i) $x, -y+1/2, z$; (ii) $-x+2, -y, -z+1$; (iii) $-x+2, y+1/2, -z+1$; (iv) $-x+2, y+1/2, -z+2$; (v) $-x+2, -y, -z+2$.

chemical units, a $\{[(PO_4)_2(VO)_2(H_2O)_2]^-\}_n$ 2-D mesh (figure 3, heavy lining); the highly symmetric mesh is formed by concatenated $P_2V_2O_4$ loops of different symmetry. Those bisected by $y=0$ or $y=1/2$ planes have -1 symmetry; while the ones at $y=1/4$ or $y=3/4$ are bisected by the m plane of the $P2_1/m$ S.G. The Cu(II) + O3W group "decorates" this basic array through binding alternatively from above and below the plane, completing the octahedral coordination of Cu(II) (figure 3, hollow lining) by face-, edge and corner-sharing with the VO_6 polyhedra. This linkage leads to metal···metal distances of Cu1···V1 2.978(2); Cu1···V2: 3.557(2) Å. Coordination also reflects in the phosphate geometry, where the P–O12 bond involving the doubly coordinated O12 is sensibly longer than the remaining three P–O bonds (table 2).

The strongly connected 2-D structures stack along [100] and are connected by water-mediated H-bonds involving O1W and O3W as donors (figure 4, table 3). O2W does not seem to be involved in any important interaction of the sort, and as a result its hydrogen atoms appear rather blurred (and thus not trustable identifiable) in the difference map.

3.3. *Magnetism*

Figure 5 shows $\chi_M T$ *versus* T for $[Cu(VO)_2(PO_4)_2(H_2O)_4]_n$. At 300 K, the value $\chi_M T$ is 1.09 $cm^3 mol^{-1} K$, close to that expected for three uncorrelated S = ½ spins (1.125 $cm^3 mol^{-1} K$ for one Cu(II) and two VO(II)). Upon cooling, $\chi_M T$ decreases slowly, but under 60° it decreases abruptly, indicating an antiferromagnetic interaction (irregular points about 60°C are due to random experimental errors).

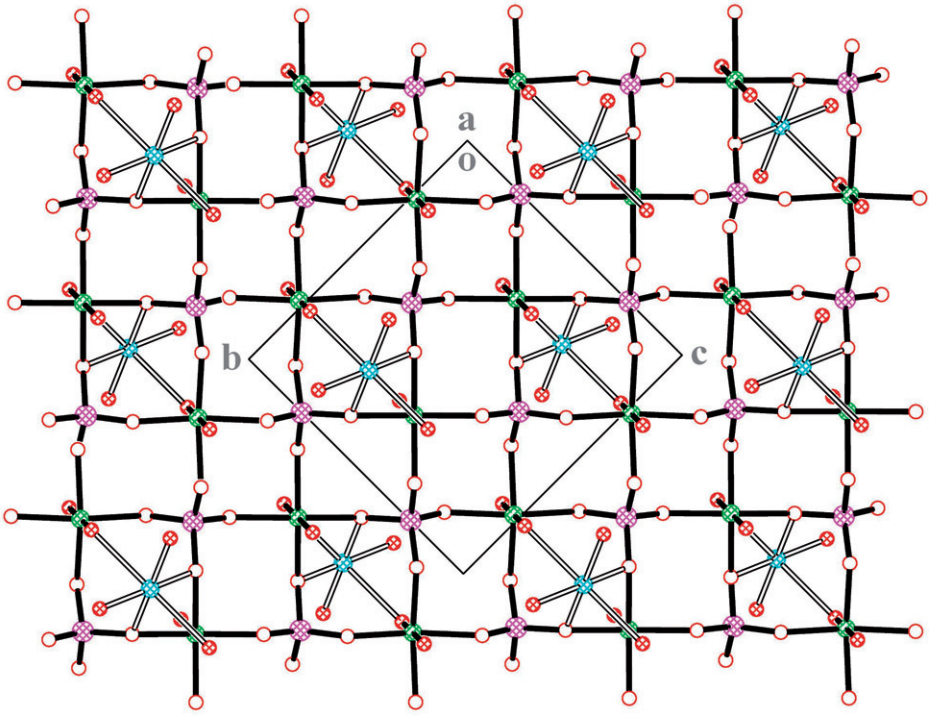

Figure 3. Packing view of **1** drawn along the [100] direction showing the (100) 2-D mesh and the elementary loops (A, B) building it up. Hydrogen atoms have been omitted for clarity.

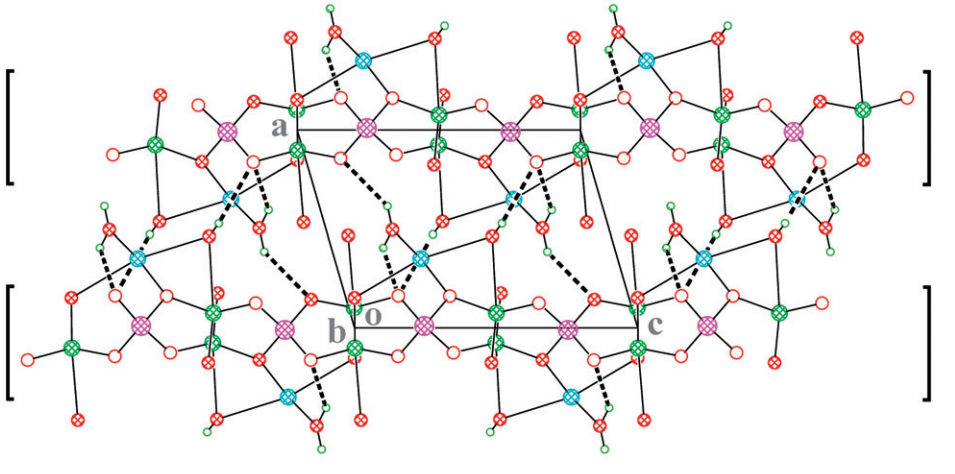

Figure 4. A side view of the (100) planes (in brackets), projected down [010], showing the way in which they pile up. H-bonds are broken lines.

3.4. *Magnetic model*

Based on the molecular structure, the magnetic system can be visualized as three paramagnetic centers (one copper(II) and two V(IV)) in an irregular triangular

Table 3. Hydrogen-bond geometry for **1** (Å, °).

D–H···*A*	*D*–H	H···*A*	*D*···*A*	∠*D*–H···*A*
O1*W*–H1*W*···O14^{vi}	0.85(2)	2.35(2)	3.075(10)	143(3)
O3*W*–H3*WA*···O13^{vii}	0.85(2)	2.09(4)	2.900(9)	158(9)
O3*W*–H3*WA*···O11^{vii}	0.85(2)	2.18(8)	2.822(8)	132(9)
O3*W*–H3*WB*···O14	0.85(2)	1.95(6)	2.688(9)	144(9)

Symmetry codes: (vi) $-x+1, -y, -z+1$; (vii) $x-1, y, z$.

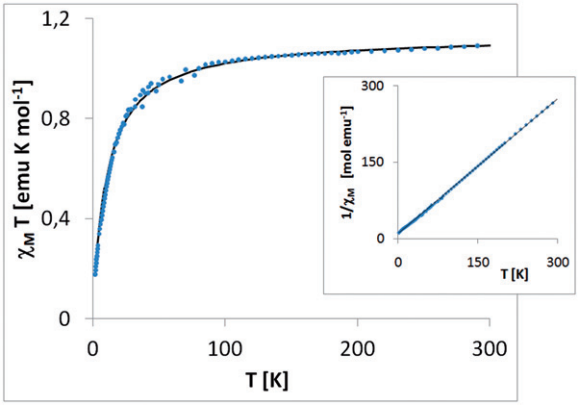

Figure 5. Magnetic behavior of **1**.

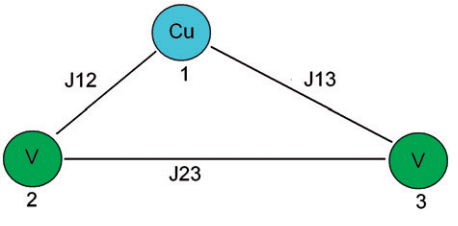

Scheme 1. Irregular triangular arrangement for the paramagnetic centers.

arrangement [18, 19] (scheme 1). Accordingly, an unsymmetrical trinuclear model was used to fit the magnetic data. The original isotropic spin Hamiltonian for this model is

$$\hat{H} = J_{12}\hat{S}_1 \cdot \hat{S}_2\hat{S}_2 + J_{13}\hat{S}_1 \cdot \hat{S}_3 + J_{23}\hat{S}_2 \cdot \hat{S}_3$$

where J stands for the exchange-coupling. The interactions between three local doublets (one copper(II) and two vanadium(IV)) lead to a quartet and two molecular doublets. The microstates are formed by the basis set $|M_{S1}, M_{S2}, M_{S3}|$.

The component $M_S = 3/2$ of the quartet state is $|1/2,1/2,1/2|$ and the energy of this state is given by

$$\begin{aligned} E(3/2) &= \langle 1/2, 1/2, 1/2|H|1/2, 1/2, 1/2\rangle \\ &= -(J_{12} + J_{13} + J_{23})/4 \end{aligned}$$

The analysis for $M_S = 1/2$ give us

$$E(1/2, \pm) = \frac{(J_{12} + J_{13} + J_{23})}{4} \pm \frac{\sqrt{(J_{12} - J_{23})^2 + (J_{23} - J_{13})^2 + (J_{13} - J_{12})^2}}{8}$$

The relative energies of the three states depend on only two energy gaps, Δ_1 and Δ_2 defined by

$$\Delta_1 = E(1/2, -) - E(1/2, +)$$
$$\Delta_2 = E(3/2) - E(1/2, +)$$

The three interaction parameters cannot be determined unequivocally from the magnetic data. A simplifying hypothesis must be made, for instance assuming that one of the parameters is negligible with respect to the other two due to the structure of the trinuclear unit. The magnetic susceptibility may be expressed *versus* Δ_1 and Δ_2 as follows:

$$\chi_{\mathrm{M,trimer}} = \frac{N\beta^2}{4k(T-\theta)} \left[\frac{g_{1/2,+}^2 + g_{1/2,-}^2 \exp(-\Delta_1/kT) + 10 g_{3/2}^2 \exp(-\Delta_2/kT)}{1 + \exp(-\Delta_1/kT) + 2\exp(-\Delta_2/kT)} \right] \quad (1)$$

where θ accounts for the interaction between trimeric units; $g_{1/2,+}$, $g_{1/2,-}$, $g_{3/2}$ are the molecular g-factors.

The best fit leads to $g_{1/2,+} = 1.94$, $g_{1/2,-} = 1.89$, $g_{3/2} = 1.91$, $\Delta_1 = 26.6\,\mathrm{cm}^{-1}$, $\Delta_2 = 13.5\,\mathrm{cm}^{-1}$, and $\theta = 11.13\,\mathrm{K}$ with $R = 1.9\ 10^{-4}$, defined as follows. J values thus obtained are: $J_{12} = -17$, $J_{13} = 13$, and $J_{23} = 0\,\mathrm{cm}^{-1}$.

$$R = \frac{\sum \left[(\chi_{\mathrm{M}} T)_{\mathrm{obs}} - (\chi_{\mathrm{M}} T)_{\mathrm{cal}} \right]^2}{\sum \left[(\chi_{\mathrm{M}} T)_{\mathrm{obs}} \right]^2} \quad (2)$$

The general theory of magnetism describes the final value of J as the result of competition between antiferromagnetism, AFM, and ferromagnetism, FM, (equation (3)):

$$J = \mathrm{AFM} + \mathrm{FM} \quad (3)$$

Both factors depend on the distance between magnetic orbitals and other variables; while the AFM depends on the sign and overlap between magnetic orbitals, the FM depends only on this overlap.

Kahn [16, 17] described a similar situation where the interaction between copper and vanadium is similar to the more important relationships discussed in this work (Cu–J12–V). For the Kahn system, the square-copper(II) and square-vanadium(IV) moieties (figure 6a) result in a flat angle ($\alpha = 180°$). In this case, the overlap occurs over a high percentage and due to the orbital sign, the final effect is zero. In this way, the AFM is cancelled and only the FM contribution survives.

In our case the effect of the sign is similar, but due to an alpha angle of 135.4° the overlap between copper and its nearest vanadium is weak, but not zero; therefore the antiferromagnertic interaction is the main one and ferromagnetism in this couple becomes negligible (figure 6b). The next nearest vanadium (joined through the oxygen atoms of the phosphate group) represents a weaker, though important, contribution because it helps in describing the asymmetric triangle (a dimeric model is not correct to describe this system).

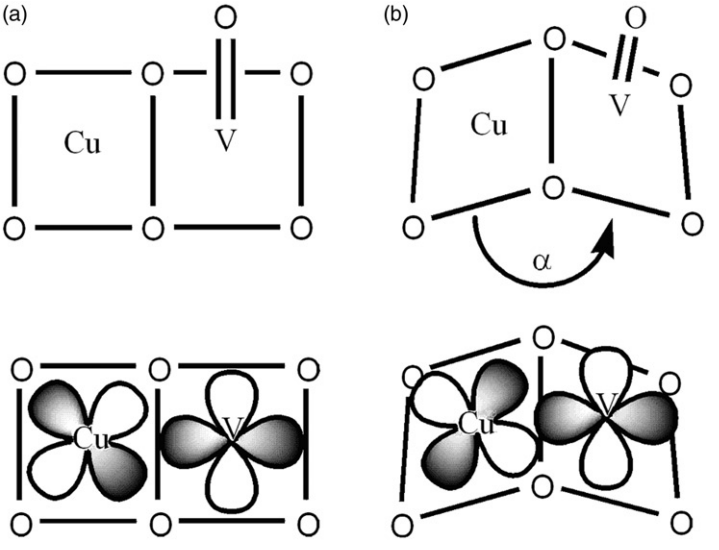

Figure 6. Dihedral angle between the square-copper(II) and the square-vanadium(IV) moieties: (a) the plane angle on the Kahn system; (b) $\alpha = 135.4^{\circ}$, in this work.

Zheng and Lii [27] described a similar compound, $Ni(VOPO_4)_2 \cdot 4H_2O$. In this case the interaction between magnetic centers is ferromagnetic. The structure consists of $VOPO_4$ layers linked by NiO_6 octahedra. Again, the symmetry is an important factor in understanding the magnetic behavior.

3.5. *Chemometric analysis*

From the results of the multivariate analyses, a polynomial response to crystal amount was obtained for the analyzed variables (equation (4)), which considers the relative importance of the different terms. The coefficients were scaled and centered. In this polynomial, the error is the confidence intervals at 95%.

$$Y\% = 163(\pm 25.5) + 59.6X_1(\pm 23.8) - 28.0X_2(\pm 23.8) - 0.387X_3(\pm 23.8) - 38.08X_1^2(\pm 34.9) \quad (4)$$

Considering the first-order coefficients of each variable, it can be concluded that the effect of V_2O_2 (X_1) concentration is higher than the reaction temperature. This positive coefficient implies that there is a positive dependence of the crystal amount obtained (Y). The cooling rate coefficient was not significant ($p = 0.972$), for this reason this variable was not considered for the data analysis. The negative second-order coefficient for V_2O_2 (X_1^2) indicates a maximum region. There were no significant coefficients of the interaction between the variables, therefore all of them are independent.

The polynomial model was validated through an ANOVA test with 95% confidence level, where the results obtained from the experimental design were compared with the response predicted by the polynomial (table 4).

Table 4. Experimental design with the predicted responses by the polynomial.

V_2O_5 (mol) $X1$	T (°C) $X2$	Cooling rate (°C h^{-1}) $X3$	Experimental results (g)	Predicted results (g)
0.25 (−1)	130 (−1)	2.5 (0)	147.8	93.9
0.5 (+1)	130 (−1)	2.5 (0)	220.4	213.1
0.25 (−1)	150 (+1)	2.5 (0)	23,7	37.8
0.5 (+1)	150 (+1)	2.5 (0)	164.3	157.0
0.25 (−1)	140 (0)	1 (−1)	34	66.0
0.5 (+1)	140 (0)	1 (−1)	162.5	185.0
0.25 (−1)	140 (0)	4 (+1)	58	65.9
0.5 (+1)	140 (0)	4 (+1)	193	185.1
0.375 (0)	130 (−1)	1 (−1)	174	191.6
0.375 (0)	150 (1)	1 (−1)	178.3	135.5
0.375 (0)	130 (−1)	4 (+1)	171.5	191.6
0.375 (0)	150 (+1)	4 (+1)	123.2	135.5
0.375 (0)	140 (0)	2.5 (0)	133.5	163.5
0.375 (0)	140 (0)	2.5 (0)	184.3	163.5
0.375 (0)	140 (0)	2.5 (0)	180	163.5

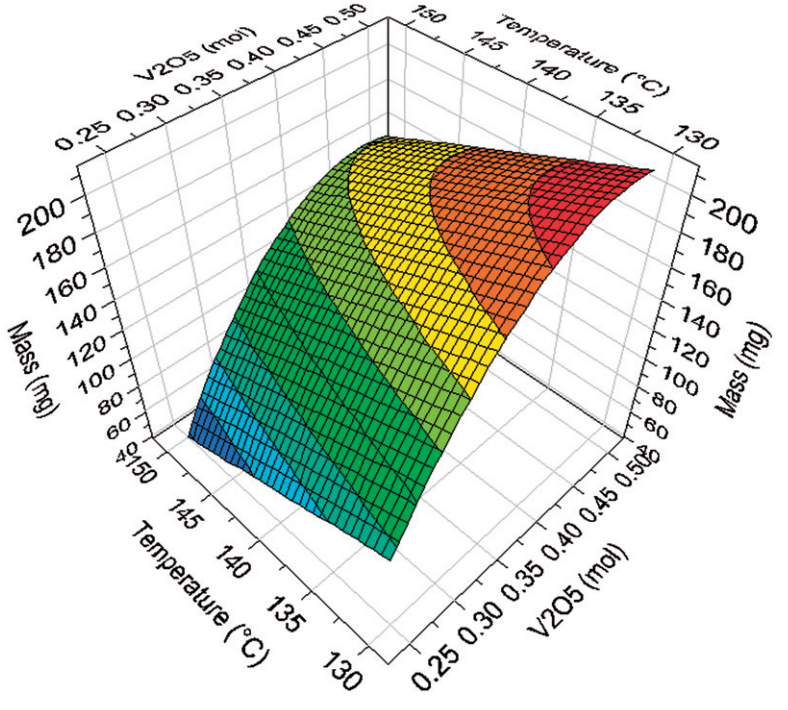

Figure 7. Surface plots of polynomial response.

There are no significant differences between the calculated and the experimental values. In this way, the R^2 value of linear regression was 0.814, indicating a validated prediction from the response polynomial.

The surface plots of the polynomial response are shown in figure 7. The regions of maximal crystal mass are shown by a layer over 200 mg. This maximum region can be

observed at V_2O_5 ranging from 0.40 to 0.50 mol (limit of the function domain) and temperature from 130°C (limit of the function domain) to 135°C.

Through a SIMPLEX analysis over the response surface, the optimal values for crystal mass were obtained: V_2O_5 mol = 0.5, temperature = 130°C. With these values the predicted crystal mass from the polynomial is 213 ± 41.2 mg, considering the 95% confidence interval.

4. Conclusions

The $[Cu(VO)_2(PO_4)_2(H_2O)_4]_n$ compound presents paramagnetic behavior with $\chi_M T = 1.09\,cm^3\,mol^{-1}K$, close to that expected for three uncorrelated $S = ½$ spins; however, it is found that at low temperatures an antiferromagnetic interaction is dominant. The magnetic system is constituted by three paramagnetic centers: one copper(II) and two V(IV) in an irregular triangular arrangement. A weak cooperative interaction is the result of competition between ferro and antiferromagnetism of their paramagnetic centers, in which the former interaction is the main one.

The analytical method, RSM, is valid to optimize experimental conditions in the hydrothermal synthesis of $[Cu(VO)_2(PO_4)_2(H_2O)_4]$ system. The theoretical crystal yield is in agreement with the experimental values.

Supplementary material

CCDC 872160 contains the supplementary crystallographic data for this article. These data can be obtained free of charge from The Cambridge Crystallographic Data Centre via www.ccdc.cam.ac.uk/data_request/cif.

Acknowledgments

We acknowledge the Spanish Research Council (CSIC) for providing us with a free-of-charge license to the CSD system: CNRS-CONICYT 176, CIPA and DIUC 211.021.031-1.0-Universidad de Concepcion projects; Dr Rousnel Thyerry of Science Chimie de Rennes, Universite de Rennes-1, for the X-ray measurements.

References

[1] J. Jiménez-Jiménez, M. Algarra, E. Rodríguez-Castellón, A. Jiménez-López, J.C.G. Esteves da Silva. *J. Hazard. Mater.*, **190**, 694 (2011).
[2] A.K. Cheetham, G. Férey, T. Loiseau. *Angew. Chem. Int. Ed.*, **38**, 3268 (1999).
[3] Y. Moreno, A. Vega, S. Ushak, R. Baggio, O. Peña, E. Le Fur, J.Y. Pivan, E. Spodine. *J. Mater. Chem.*, **13**, 2381 (SCI:2.736) (2003).
[4] M.I. Khan, R.C. Nome, N.R. Putrevu, J.H. McNeely, B. Cage, R.J. Doedens. *Inorg. Chim. Acta*, **363**, 4307 (2010).

[5] J.-Y. Pivan, E. Le Fur. *J. Mater. Chem.*, **9**, 2589 (1999).
[6] C.M. Wang, Y.L. Chuang, S.T. Chuang, K.H. Lii. *J. Solid State Chem.*, **177**, 2305 (2004).
[7] Y. Moreno, G. Cárdenas, A. Tissot, O. Peña, J.-Y. Pivan, R. Baggio. *Inorg. Chem.*, **47**, 2334 (2008).
[8] W. Ouellette, B.-K. Koo, E. Burkholder, V. Golub, C.J. O'Connor, J. Zubieta. *Dalton Trans.*, 1527 (2004).
[9] G. Centi, F. Trifiro, J.R. Ebner, V.M. Franchetti. *Chem. Rev.*, **88**, 55 (1998).
[10] D. Papoutsakis, J.E. Jackson, D.G. Nocera. *Inorg. Chem.*, **35**, 800 (1996).
[11] J.T. Vaughey, W.T.A. Harrison, A.J. Jacobson, D.P. Goshorn, J.W. Johnson. *Inorg. Chem.*, **33**, 2481 (1994).
[12] P. DeBurgomaster, H. Liu, C.J. O'Connor, J. Zubieta. *Inorg. Chim. Acta*, **363**, 330 (2010).
[13] J.-Y. Pivan, E. Le Fur. *Mater. Res. Bull.*, **34**, 1117 (1999).
[14] P.M. Forster, P.M. Thomas, A.K. Cheetham. *Chem. Mater.*, **14**, 17 (2002).
[15] E. Le Fur, O. Pena, J.-Y. Pivan. *J. Mater. Chem.*, **9**, 1029 (1999).
[16] O. Kahn. *Molecular Magnetism*, Wiley-VCH, New York (1993).
[17] O. Kahn. *Angew. Chem. Int. Ed. Engl.*, **24**, 834 (1985).
[18] A. Rabenau. *Angew. Chem. Int. Ed. Engl.*, **24**, 1026 (1985).
[19] R. Walton. *Chem. Soc. Rev.*, **31**, 230 (2002).
[20] D. Contreras, Y. Moreno, Y. Salgado, G. Cardenas, R. Baggio, O. Pena, J.-Y. Pivan. *New J. Chem.*, **31**, 1751 (2007).
[21] G.E.P. Box, D.W. Behnken. *Technometrics*, **2**, 455 (1960).
[22] B. Barros, S. Scarminioi, R.E. Bruns. *Como Fazer Experimentos: Pesquisa e Desenvolvimento na Ciência e na Indústria*, Bookman, Campinas, Brazil (2001).
[23] Bruker. *SMART, V5.624. Data Collection Software*, Siemens Analytical X-ray Instruments Inc., Madison, WI, USA (2001).
[24] Bruker. *SAINT, V6.22A (Including SADABS). Data Reduction Software*, Siemens Analytical X-ray Instruments Inc., Madison, WI, USA (2002).
[25] G.M. Sheldrick. *Acta Cryst. A*, **64**, 112 (2008).
[26] A.L. Spek. *J. Appl. Cryst.*, **36**, 7 (2003).
[27] L.-M. Zheng, K.H. Lii. *J. Solid State Chem.*, **137**, 77 (1998).